Int. J. Electrochem. Sci., 16 **(2021)** Article Number: 21119, doi: 10.20964/2021.11.24

International Journal of
ELECTROCHEMICAL
SCIENCE
www.electrochemsci.org

Study of Corrosion Pit Propagation in Aluminum by Numerical Simulation using the Finite Element Method

Meriyem Mouloudi[1,], Rachid Radouani[1], Mohamed Essahli[1], Mohammed Chafi[2] and Mostafa Chhiba[3]*

[1] Hassan First University of Settat, Faculty of Science and Technology, Laboratory of Applied Chemistry and Environment, BP 577, Morocco
[2]L Hassan II University of Casablanca, Higher School of Technology, Laboratory of Chemical Engineering and Environment, BP 8012, Oasis Casablanca, Morocco
[3] Hassan First University of Settat, Faculty of Science and Technology, Radiations materials & instrumentations Laboratory, BP 577, Settat, Morocco
[*]E-mail: m.mouloudi@uhp.ac.ma

Received: 3 July 2021 / *Accepted:* 28 August 2021 / *Published:* 10 October 2021

Pitting corrosion is a localized form of corrosion that can restrict the lifetime of a metal. Studying the pitting corrosion is required to predict and prevent the risk of damage of metals susceptible to corrosion. This paper presents a finite element numerical simulation of the pit growth by illustrating the impact of hydrochloric acid concentration and the influence of the pit radius. The obtained results illustrate that the pit propagation in a chloride environment is significantly impacted by the chloride concentration and the radius of the pits. Furthermore, these results are discussed in comparison with those published in the literature.

Keywords: Finite element method, pitting corrosion, chloride, aluminum, corrosion modelling.

1. INTRODUCTION

Aluminum has economic and industrial importance due to its chemical and physical properties such as its low density, its resistance to corrosion and its high electrical and thermal conductivities [1]. However, previous studies on aluminum corrosion have shown that it is sensitive to pitting corrosion when it is exposed to an aggressive environment [2-6]. This may significantly restrain its lifetime.

The pitting corrosion is a localized form of corrosion affecting most often metals and alloys in a passive state [7]. Losing local integrity of the passive film [8] under the effect of some aggressive anions such as halogens and chlorides [9,10], may cause an initiation and a propagation of pitting corrosion. Generally, the size of the pits ranges from nano to millimeter and the majority of the

metallic surface remains intact [11]. The difficulties related to the small size of the pits and the complexity of the pitting corrosion phenomenon may restrict the understanding of the physical, chemical and electrochemical process of this type of corrosion.

Nowadays, new methods have been developed as an alternative to experimental methods. Numerical simulation based on the finite element method is a suitable solution to predict the rate of pitting corrosion propagation in various metals that are exposed to diverse environments.

In fact, the pitting corrosion models developed by numerical simulation in the literature have been made on Iron or Steel [12-14], and there are some works that are made to study the pitting corrosion of aluminum and its alloys [9, 10, 15, 16,17, 18].

The numerical simulations that have been applied on aluminum and its alloys reported on the local chemistry of the pitting. As an example, Verhoff and Alkire [16,17] have studied the anodic dissolution on pure aluminum in a chloride environment at a pH of 11 for a hemispherical pitting case.

Further, Guseva [9,10] has suggested two models, the first one concerns the simulation of passive aluminum surface with pitting and the second one related to the temporal evolution of the local chemical environment during the initial phase of localized corrosion of AA2024 aluminum alloys. Also, Abodia [20] developed a model to provide understanding the steps in initiation of pitting in AA2024. Another model of localized corrosion of aluminum alloys with a mobile boundary has been proposed by Xiao and Chaudhuri [15] to simulate the evolution of pitting morphology.

Furthermore, CFD has been used to determine the distribution of attack on aluminum electrode surface during its dissolution in the Electrocoagulation reactor [19].

In this work, a numerical simulation of two-dimensional growth of a corrosion pitting on the aluminum surface was studied using Comsol Multiphysics software. The objective is to demonstrate the impact of the electrolyte, specifically the hydrochloric acid concentration, and the influence of the geometry, notably the pit radius R_{pit}, on the potential distribution of the electrolyte and the corrosion rate of aluminum along the pitting area. The numerical results have been compared to the experimental data and extensively discussed.

Despite the large deployment and significant enthusiasm of pitting corrosion studies, in particular chloride caused pitting, for protection of aluminum, to our knowledge there have been very few attempts of integrated computation of corrosion to directly correlate the distribution of electrolyte potential, the pitting shape, the pitting radius to hydrochloric acid concentration. Such validation is hypothetically essential to predict the pitting phenomenon by mean of computational modeling with aggressive medium properties.

2. MATERIAL AND METHOD

2.1. Material and geometry

In this paper, we have opted for aluminum as a metal. Since it is sensitive to pitting corrosion, due to a local degradation of the oxide film in a highly corrosive environment [21].

Pits forms vary considerably, as illustrated in Figure 1, and are generally saucer-shaped, conical or hemispherical [11].

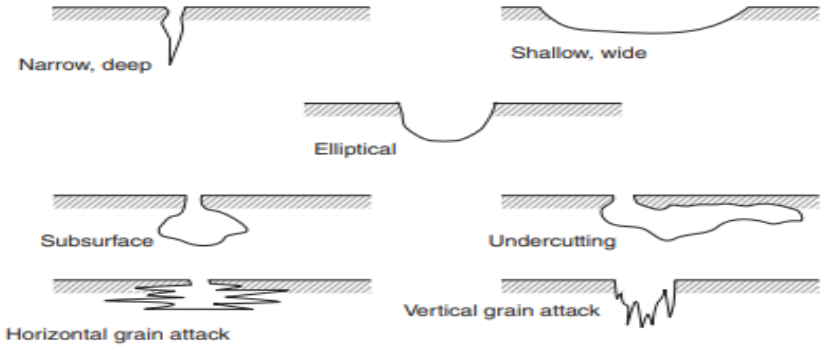

Figure 1. The shapes of corrosion pits.

We executed our numerical simulation on a 200 µm × 400 µm rectangular area with a hemispherical pitting of radius R_{pit}= 20 µm inserted on the middle of the bottom border. These parameters of size and shape are similar to natural corrosion pits that were detected in a chloride solution [22,23].

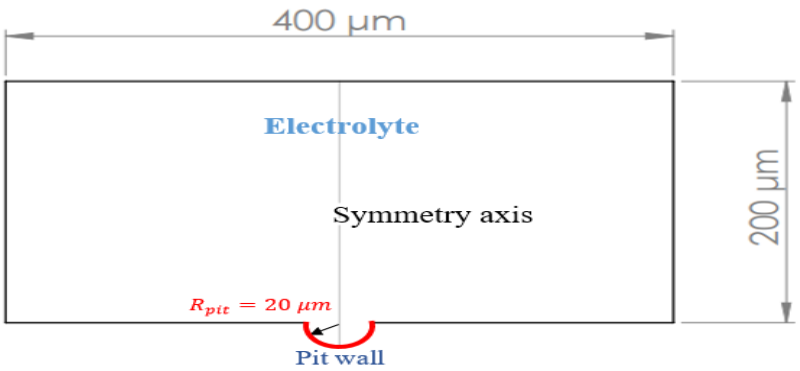

Figure 2. The characteristics of the 2D pitting geometry.

2.2. Governing equations

In this study, the process of electrochemical corrosion at the corrosion pitting interface is simulated using numerical equations with experimentally obtained corrosion parameters.

For constant conductivity, the potential distribution in the electrolyte is driven by Laplace's equation [12, 22] presented as follows:

$$\nabla^2 \emptyset = 0 \qquad (1)$$

Where ∇^2 is the Laplacian operator and $\emptyset$ is the electric potential (V).

An appropriate boundary condition involving the electric potential on the metal-electrolyte interface is required to solve the Laplace equation. This boundary condition can be defined in terms of the potential flux as a function of the dissolution current density according to the following equation [12]:

$$\nabla \emptyset . \boldsymbol{n} = \frac{i(\emptyset)}{\sigma_c} \qquad (2)$$

Where $\boldsymbol{n}$ is the unit normal at the interface, i is the anodic current density (A/m^2); σ_c is the electrical conductivity of the electrolyte (S/m).

In this work, we consider only the anodic reaction ($M_{(s)} \rightarrow M_{(aq)}^{n+} + ne^-$) that controls the dissolution of metal on pitting corrosion. The corrosion rate is expressed as a function of the current density as follows [25,26]:

$$i_a = i_0 \exp\frac{\alpha n F \eta}{RT} \qquad (3)$$

Where i_0 is the exchange current; $F$is the Faraday constant; n is the charge number of the dissolving reactant; α is the transfer coefficient; R is the gas constant; T is the temperature; η is the overpotential with $\eta = E - E_e$; E is the applied potential and E_e is the equilibrium potential.

This equation is obtained from the Butler-Volmer equation (BVe) assuming that the over potential is positive, the symmetric term of BVe with a negative exponential is not considered in this work. Therefore, the BVe is expressed by the following Tafel's law :

$$\eta = b_a \log\frac{i_a}{i_0} \qquad (4)$$

Where $b_a = 2.303\frac{RT}{\alpha n F}$ is the anodic Tafel slope. This parameter can be measured experimentally.

2.3. Boundary conditions

The non-corrosive boundaries were applied to the electrolyte exterior limits and electrode domains as shown in Figure 4.

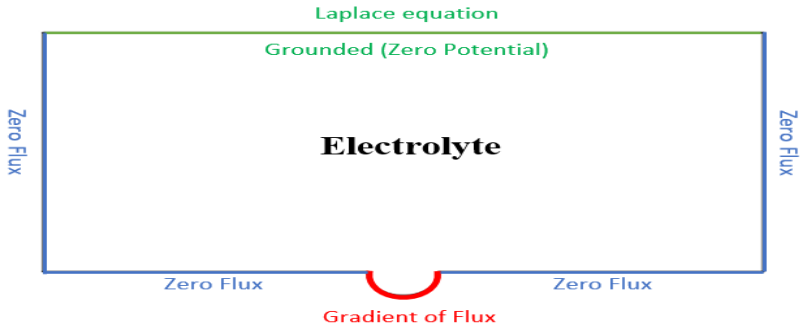

Figure 3. Boundary conditions.

The geometrical deformation of non-corrosive boundary is null. The model does not contain a passive film and the analysis is done at equal ambient temperature (298.15 K).

2.4. Method and parameters of the study

Solving the governing equations by numerical simulation based on the finite element method requires the determination of the electrochemical parameters and the characteristics of the electrolyte.

In this study, we have shown the impact of the electrolyte and the influence of the pitting geometry on the potential distribution and the corrosion rate of aluminum.

2.4.1. Effect of the electrolyte

In this part, we simulated corrosion pitting in the hydrochloric acid concentrations as follows: 0.5, 1, 1.5, 2 and 2.5 HCl M. The electrochemical parameters used and the conductivity for the above concentrations are listed in Table 1.

Table 1. Electrolyte conductivity [27] and electrochemical parameters [28].

Concentration (M)	**Conductivity (S/m)**	**E_{corr} (mV)**	**i_{corr} (mA/cm^2)**	**b_a (mV)**
HCl 0.5	18.035	-770	0.882	102
HCl 1.0	33.2	-790	1.68	115
HCl 1.5	45.87	-825	8	124
HCl 2.0	56.28	-830	13.6	147
HCl 2.5	59.4	-840	15	168

2.4.2. Influence of the pit geometry

The influence of the pit geometry on the potential and corrosion rate of aluminum is studied only in HCl 1M including the variation of the pit radius R_{pit} from 10 µm to 50 µm with a 10 µm step.

3. RESULTS AND DISCUSSION

After applying the governing equations, boundary conditions and mesh for the geometry predefined in Figure 2, the results obtained are presented and discussed below.

3.1. Effect of the electrolyte

3.1.1. Electrolyte potential

The resolution of Laplace's equation allowed us to present the electrolyte potential on the pitting surface in the hydrochloric acid concentrations indicated in Table 1. The results of the simulation are shown in Figure 4.

From Figure 4, it is clear that the electrolyte potential changes in the same way as the electrolyte concentration:

E (HCl 2.5 M) >*E* (HCl 2 M) >*E* (HCl 1.5 M) >*E* (HCl 1 M) >*E* (HCl 0.5 M)

These results concur with the previous work done by Mai and Soghrati [29] in which they confirmed that increasing the concentration of NaCl leads to an increase in the conductivity of the electrolyte, thereby reducing the Ohmic potential drop and accelerating the corrosion of the metal.

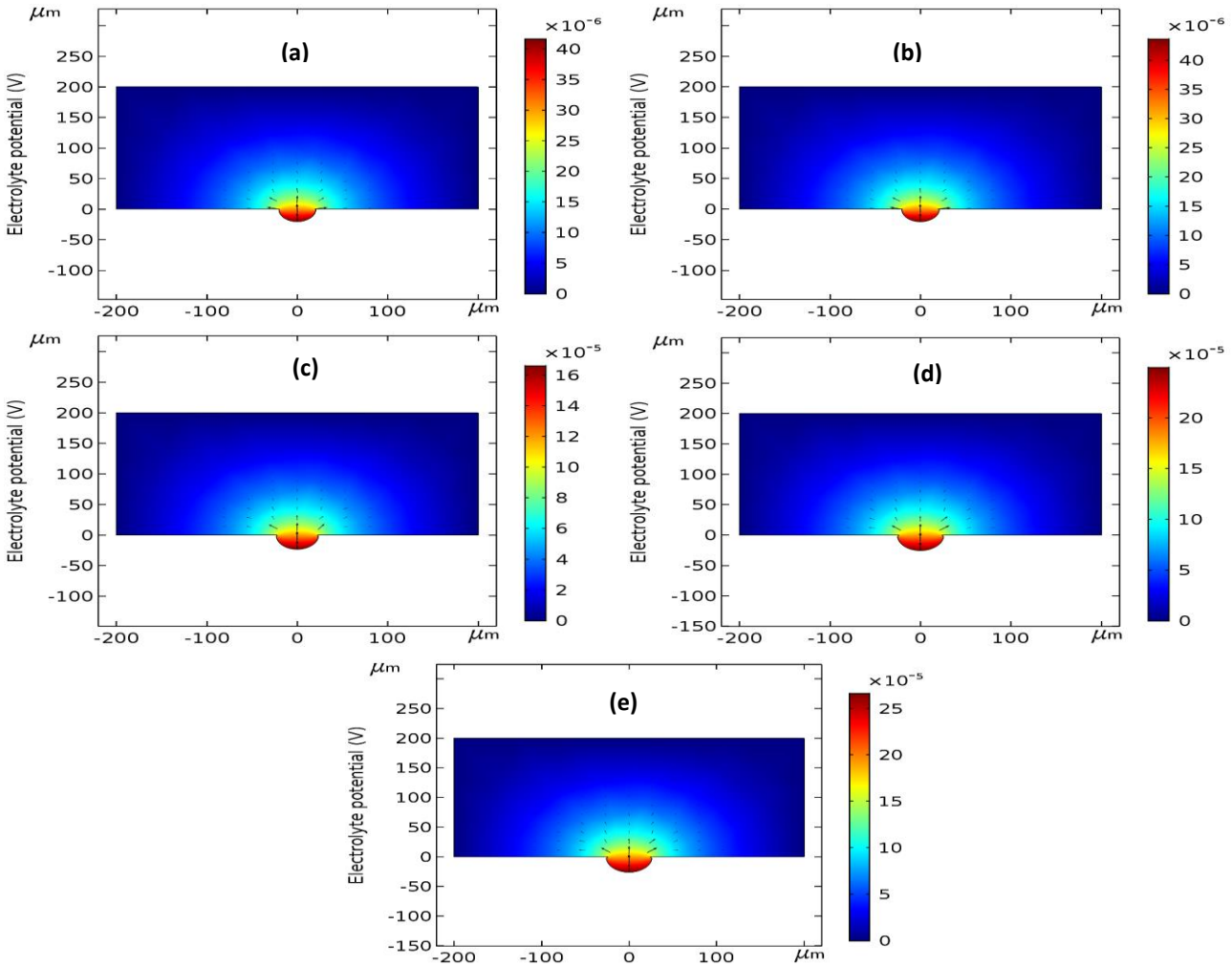

Figure 4. Electrolyte potential at 1200s with deformed geometry. (a) 0.5, (b) 1.0, (c) 1.5, (d) 2.0, (e) HCl 2.5 M.

3.1.2. Evolution of the pit morphology

The corrosion pitting growth simulation was done to follow the evolution of pit-morphology during dissolution process inside the pit in the concentrations of hydrochloric acid previously mentioned. Figure 5 illustrates the evolution of the pit morphology as a function of hydrochloric acid concentrations.

The chloride ions are necessary for the growth of pits as proved by Hunkeler and Boehni [4]; Pereira and José [31]. Moreover, it is observed that the corrosion pitting remains hemispherical throughout the growing process in hydrochloric acid solutions at different concentrations. This showed that diffusion distances are identical for all spots on the pitting border. These obtained results are in accordance with those obtained by Ernst and Newman [30]. The same behavior and morphology of pitting on pure aluminum by electrochemical and scanning electron microscope (SEM) method has been confirmed by Ren and Zuo [32].

In order to study the variation of R_{pit} as a function of concentration, the simulation results at t=1200s were extracted. The values obtained are given in Table 2.

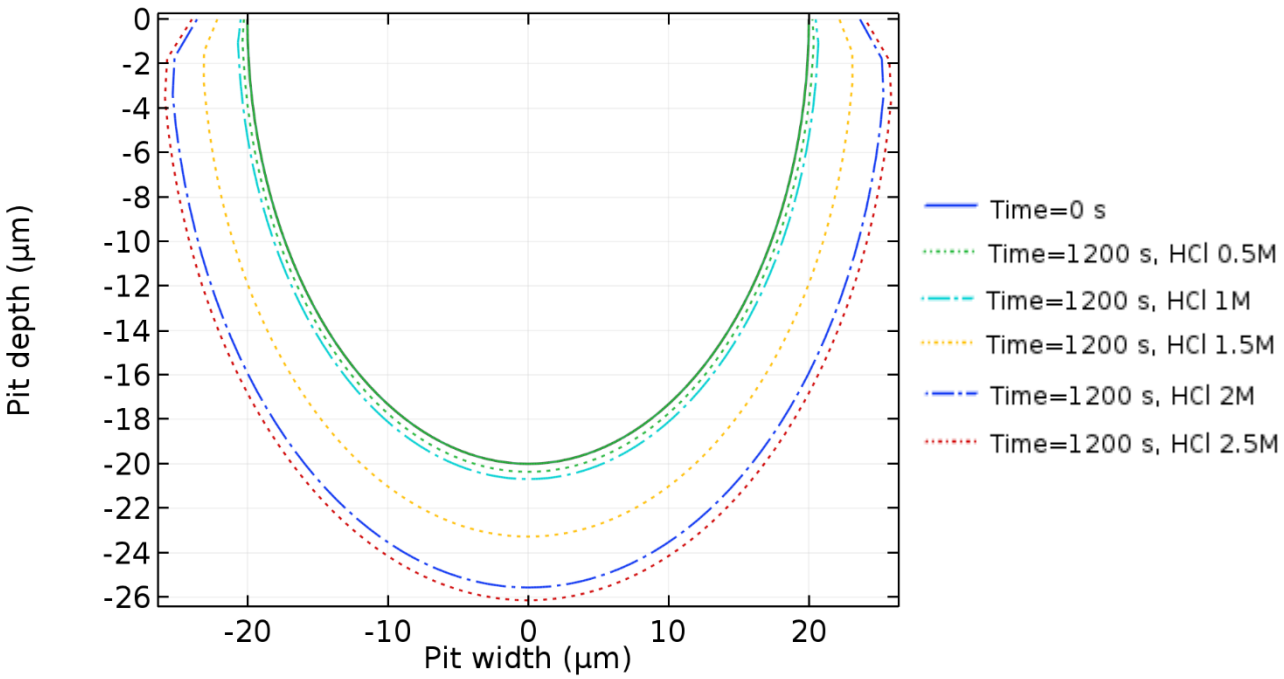

Figure 5. Pit morphology evolution of aluminum at 1200s for different hydrochloric acid concentrations at 298.15 K.

Table 2. Variation of R_{pit} with hydrochloric acid concentration at 1200s.

Concentration (M)	**R_{pit} at 1200s (µm)**
HCl 0.5	20.5
HCl 1.0	20.8
HCl 1.5	23.1
HCl 2.0	25.1
HCl 2.5	26.0

From Table 2, it can be seen that the pit radius R_{pit} increases with the hydrochloric acid concentration.

The pitting radius has the best linear correlation with acid concentration (R_{pit} = 4.3 [HCl] + 16.55 with high R^2 correlation coefficient of 0.9984, Rpit in µm and [HCl] in M) between 1.0 and 2.0 M of HCl, but when we extend acid domain between 0.5 and 2.0 M of HCl a slight linearity defect appears (R_{pit} = 3.06 [HCl] + 18.51 with high R^2 of 0.957) at both concentration extremities. The pit radius from the infinite dilution of the aggressive solution to its saturation has distinct trends with the linear one being more noticeable at moderated hydrochloric acid concentrations.

3.1.3. Corrosion rate C_R

The corrosion rate is calculated using the following relation [33]:

$$C_R = \frac{I_{corr} \times M}{z \times F \times \rho} \qquad (5)$$

Where V_c is the corrosion rate (mm/yr), I_{corr} is the corrosion current density (A/cm^2), M is the molar mass $\mathrm{M(Al)}$ = 26.98 g/mol, z is the aluminum valence z = 3, F is the Faraday constant F = 96500 A·S/mol and ρ is the aluminum density ρ = 2.7 g/cm^3. The results of the numerical simulation of the corrosion rate of aluminum are shown in Figure 6.

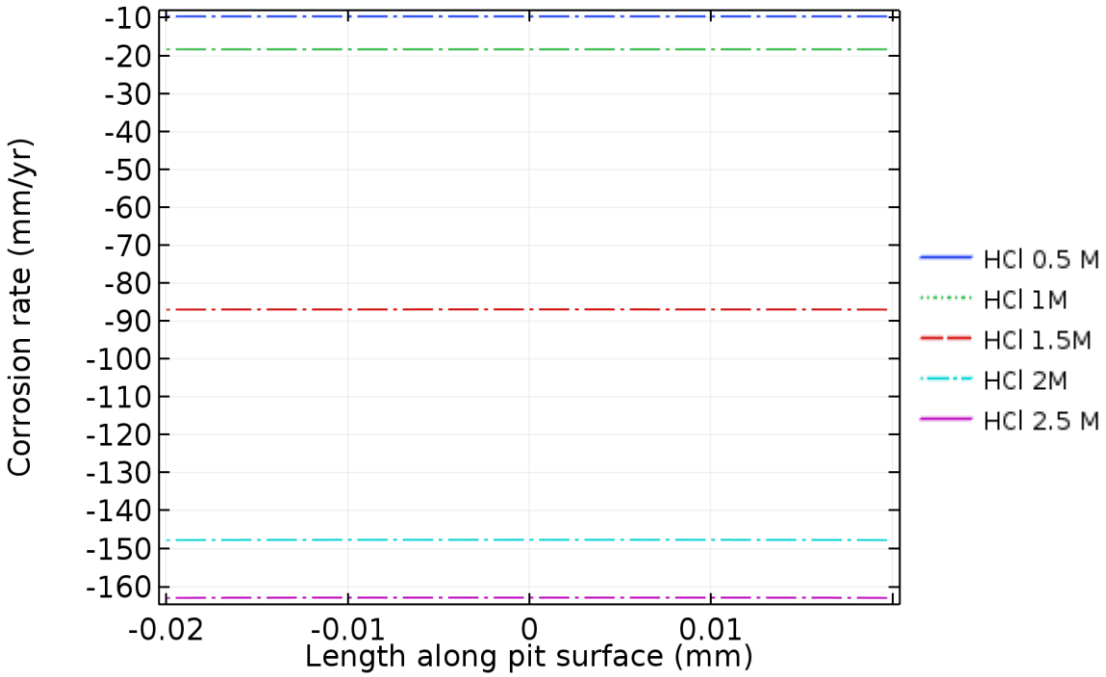

Figure 6. Corrosion rate of aluminum in mm/yr for different hydrochloric acid concentrations at 298.15 K.

These obtained results show that the corrosion rate of aluminum is increasing if the concentration of hydrochloric acid solution is increasing:

C_R (HCl 2.5 M) > C_R (HCl 2 M) > C_R (HCl 1.5 M) > C_R (HCl 1 M) > C_R (HCl 0.5 M)

This result is in agreement with those studies done by Malik [34] and Younis [35] (the authors have shown that the corrosion rate increases with the chloride concentration).

To provide more details, a comparative study of the corrosion rate of aluminum between the experimental results and the results obtained by numerical simulation was done. Table 3 shows the results of this comparison.

To compare the experimental results with the results obtained by numerical simulation, we calculated the average standard difference between the values observed experimentally and the calculated values. This deviation is 0.99 mm/yr. Furthermore, the coefficient of determination R^2 is 1. This indicates that the proposed model can predict the experimental data with a reasonable accuracy and estimate the lifetime of aluminum in the concentrations indicated in Table 3.

Table 3. Comparison of experimental and numerical simulation values of corrosion rate of aluminum in HCl 0.5 M, HCl 1 M, HCl 1.5 M, HCl 2 M and HCl 2.5 M.

Concentration (M)	Corrosion rate C_R (mm/yr)		
	Ref. [26]	This work	Deviation in %
HCl 0.5	9.7	9.6	-1.03
HCl 1.0	18.48	18.29	-1.02
HCl 1.5	88	86.99	-1.14
HCl 2.0	149.6	147.84	-1.17
HCl 2.5	165	163.09	-1.15

The corrosion rate was correlated to acid concentration, we found C_R = 129 [HCl] - 109.5 with a high R^2 correlation coefficient of 0.9984, C_R in mm/yr and [HCl)] in M) between 1.0 and 2.0 M HCl.

3.2. Influence of the pit geometry

3.2.1. Electrolyte potential

The electrolyte potential on the pitting surface was obtained by solving Laplace's equation only in the case of hydrochloric acid solution HCl 1M by including the variation of the pit radius R_{pit} from 10 µm to 50 µm with a 10 µm step. The results found are presented in Figure 7.

It can be seen that the potential increases as the pit radius increases:

E (R_{pit} =50µm) >E (R_{pit} =40µm) >E (R_{pit} =30µm) >E (R_{pit} =20µm) >E (R_{pit} =10µm)

These results can be interpreted by the fact that more R_{pit} is larger the pit is more open, which leads to easier exchange with the external environment. Similarly, Xiao and Chaudhuri [15] confirmed that the solution inside the pit is more aggressive (i.e. lower pH and higher concentration of chloride ions) with increasing pit size.

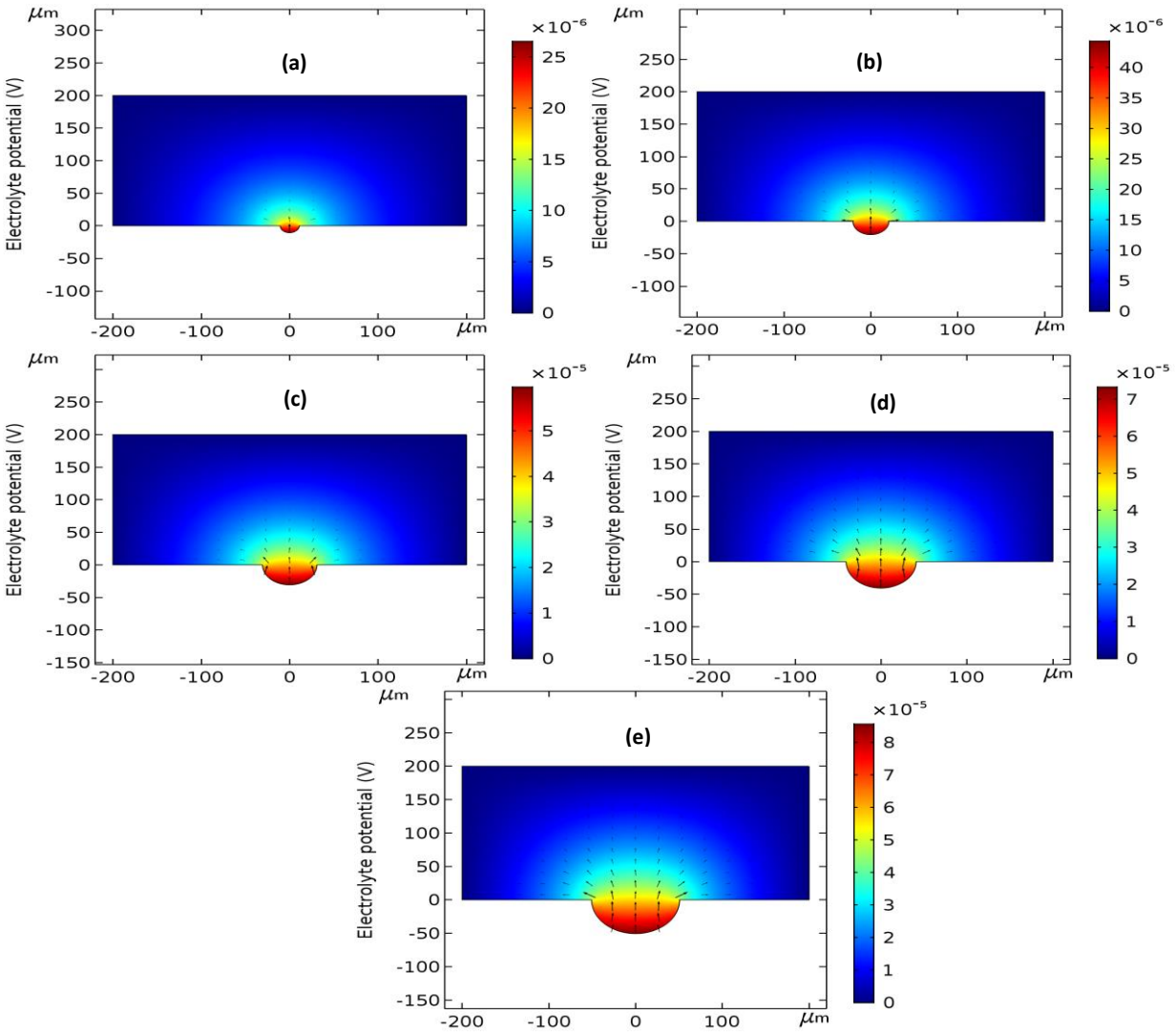

Figure 7. Electrolyte potential in HCl (1M) at 1200s with deformed geometry. (a) R_{pit}=10µm, (b) R_{pit} =20µm, (c) R_{pit} =30µm, (d) R_{pit} =40µm, (e) R_{pit} =50µm.

3.2.2. Current density

In the following step, we will present the anodic current density of aluminum along the pit wall (from the bottom to the mouth of the pit) for different pit radius R_{pit}. Figure 8 shows the obtained results.

From Figure 8, it can be clearly seen that the current density is inversely proportional to the pit radius. These results are confirmed by Tricoit [36].

Moreover for a given pit radius, we see a difference in current density between the mouth and the bottom of the pit. This deviation is even larger when the pit radius is higher. These findings are in agreement with the results in the literature [36].

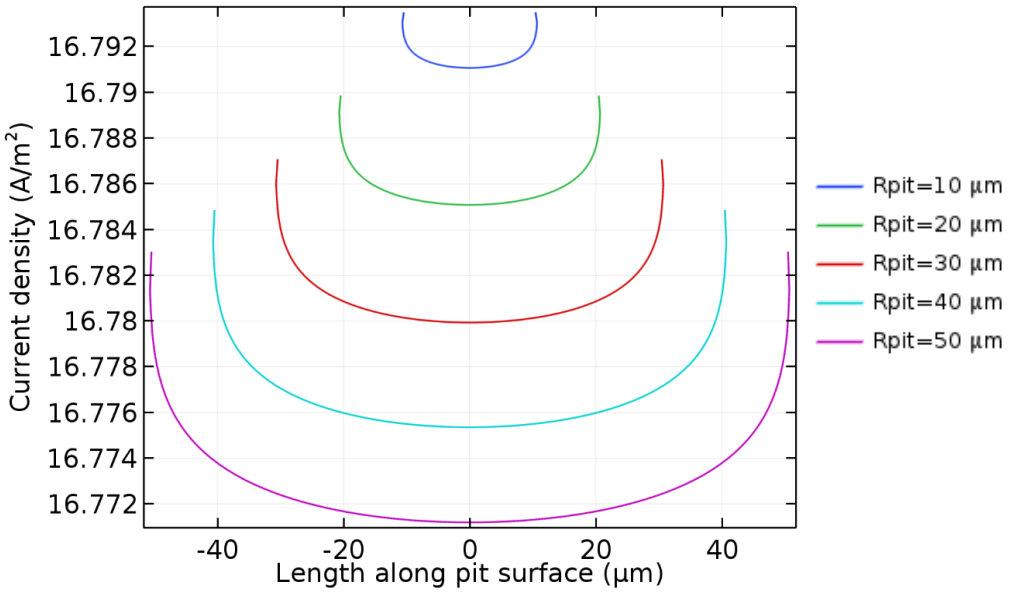

Figure 8. Anodic current density of aluminum in HCl (1M) for different pit radius R_{pit}. at 298.15 K.

3.2.3. Corrosion rate C_R

The corrosion rate along the pit wall (from the bottom to the mouth of the pitting) was illustrated in Figure 9 for different pit radius.

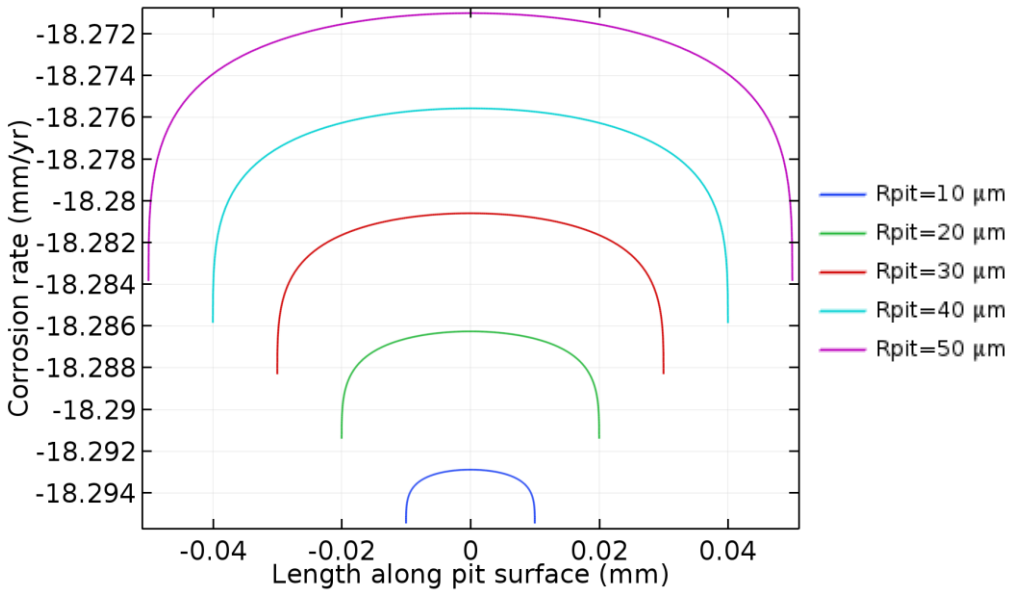

Figure 9. Corrosion rate of aluminum in HCl (1M) for different pit radius R_{pit} at 298.15 K.

From Figure 9, it can be seen that the corrosion rate along the metal wall decreases as the pit radius increases:

C_R (R_{pit} =10µm) > C_R (R_{pit} =20µm) > C_R (R_{pit} =30µm) > C_R (R_{pit} =40µm) > C_R (R_{pit} =50µm)

Furthermore, the corrosion rate of aluminum is higher at the mouth of the pit than at the bottom and the deviation is larger for the high pit radius. This is in agreement with some previous studies in the literature [36,37]. The flare observed in Figure 9 is due to the ohmic drop in the cavity as it has been studied earlier [36].

4. CONCLUSION

The pitting corrosion behavior of aluminum was studied by illustrating the influence of the electrolyte and the geometry. This was done by numerical simulation using FEM (finite element method). The main conclusions reached are as follows:

- The distribution of electrolyte potential increases with hydrochloric acid concentration and pitting radius R_{pit}.

- The pitting maintains its hemispherical shape throughout the growth process in hydrochloric acid solutions at different concentrations.

- The pitting radius R_{pit} and the corrosion rate of aluminum increase with the hydrochloric acid concentration.

- The anodic current density of aluminum is higher at the pitting edge than at the bottom of the pitting. This difference in current density is even more important when the pitting radius R_{pit} increases.

- The corrosion rate of aluminum decreases along the wall of the pit as the radius R_{pit} increases. Moreover, it is more important at the edge of the pit than at the bottom of the pit, which indicates a tendency to flare.

- The determining factor that led to this flaring in our simulations is the ohmic drop.

The results of our simulations show a good agreement with the experimental work done previously.

In this paper, we have used numerical simulation as a predictive technique to understand the behavior of aluminum against pitting corrosion in a hydrochloric acid solution. Our further work will be developing this model to understand the physical, chemical and electrochemical phenomena involved in pitting corrosion processes, considering the transportation of material and all the chemical and electrochemical reactions that can occur in aggressive environments.

References

1. J.R. David, Corrosion of aluminum and aluminum alloys, *ASM International*, (1999), USA.
2. Z. Szklarska-Smialowska, *Corros. Sci*., 41 (1999) 1743.
3. F. Sato and R.C. Newman, *Corrosion*, 54 (1998) 955.
4. F. Hunkeler and H. Boehni, *Corrosion*, 37 (1981) 645.
5. G.S. Frankel, *Corros. Sci*., 30 (1990) 1203.
6. B. Zaid, D. Saidi, A. Benzaid and *S.* Hadji, *Corros. Sci*., 50 (2008) 1841.
7. S. Jafarzadeh, Z. Chen and F. Bobaru, *Corros. Rev*., 37 (2019) 419.
8. S.M. Sharland, *Corros. Sci*., 27 (1987) 289.
9. O. Guseva, P. Schmutz, T. Suter and O. Trzebiatowski, *Electrochim. Acta*, 54 (2009) 4514.
10. O. Guseva, J.A. DeRose and P. Schmutz, *Electrochim. Acta*, 88 (2013) 821.

11. P.R. Roberge, Corrosion Engineering: Principles and Practice, *McGraw-Hill*, (2008), New York.
12. N. Kotaa, S.M. Qidwaib, A.C. Lewisb and V.G. DeGiorgib, *ECS Trans*., 50 (2013) 155.
13. S. Scheiner and C. Hellmich, *Corros. Sci.*, 49 (2007) 319.
14. S. Scheiner and C. Hellmich, *Comput. Methods Appl*., 19 (2009) 2898.
15. J. Xiao and S. Chaudhuri, *Electrochim. Acta*, 56 (2011) 5630.
16. M. Verhoff and R. Alkire, *J. Electrochem. Soc*., 147 (2000) 1349.
17. M. Verhoff and R. Alkire, *J. Electrochem. Soc*., 147 (2000) 1359.
18. El Mazyani, M. Chafi and M. Essahli, *Materials Today: Proceedings*, 37 (2021) 3882.
19. J. N. Hakizimana, B. Gourich, M. Chafi, Y. Stiriba, Ch. Vial, P. Drogui and J. Naja, *Desalination*, 404 (2017) 1.
20. L.C. Abodia, J.A. DeRoseb, S. Van Dammea, A. Demeterc, T. Suterb and J. Deconincka, *Electrochim. Acta*, 63 (2012) 169.
21. A.G. Muñoz and J.B Bessone, *Corros. Sci*., 41 (1999) 1447.
22. K.P. Wong and R.C. Alkire, *J. Electrochem. Soc*., 137 (1990) 3010.
23. S.T. Pride, J.R. Scully and J.L. Hudson, *J. Electrochem. Soc*., 141 (1994) 3028.
24. R. Radouani, Y. Echcharqy and M. Essahli, *Int. J. Corros*., 2017 (2017) 10.
25. A.J. Bard and L.R. Faulkner, Electrochemical Methods: Fundamentals and Applications, *John Wiley & Sons*, (2001), New York.
26. Z. Chen and F. Bobaru, *J. Mech. Phys. Solids*, 78 (2015) 352.
27. W.J. Hamer and H.J. DeWane, Electrolytic Conductance and the Conductances of the Hydrohalogen Acids in Water, *Natl. Stand. Ref. Data Sys., Natl. Bur. Standards*, (1970), US.
28. V. Branzoi, F. Golgovici and F. Branzoi, *Mater. Chem. Phys*., 78 (2002) 122.
29. W. Mai and S. oghrati, *Electrochim. Acta*, 260 (2018) 290.
30. P. Ernst and R.C. Newman, *Corros. Sci*., 44 (2002) 927.
31. M.C. Pereira and W.J. José, *Materials Sciences and Applications*, 3 (2012) 287.
32. J. Ren and Y. Zuo, *Surf. Coat. Technol*., 191 (2005) 311.
33. N. Perez, Electrochemistry and Corrosion science, *Kluwer Academic Publishers*, (2004), New York.
34. A.U. Malik, S. Ahmad, I. Andijani and S. Al-Fouzan, *Desalination*, 123 (1999) 205.
35. A.A. Younis, M.M.B. El-Sabbah and R. Holze, *J. Solid State Electrochem*., 16 (2012) 1033.
36. S. Tricoit and R. Oltra, Modeling and numerical simulation of the propagation of pitting corrosion of iron in chlorinated medium: contribution to the evaluation of the durability of carbon steels in geological storage conditions, *University of Bourgogne*, (2012), France.
37. S. Salleh and N. Stevens, *Journal of Engineering and Technology*, 4 (2013) 159.